Applied Energy **46** (1993) 197–214

Forced Convective Air-Cooling of Simulated Printed-Circuit Boards

W. C. Tam, C. W. Leung*

Department of Mechanical and Marine Engineering, Hong Kong Polytechnic, Hung Hom, Kowloon, Hong Kong

&

S. D. Probert

Department of Applied Energy, Cranfield University, Bedford, MK 43 0AL, UK

ABSTRACT

The considered assembly consisted of a simulated printed-circuit board (PCB), in this instance a horizontal, thermally insulting base with uniformly spaced rectangular copper bars—hereafter referred to as ribs, used to mimic the behaviour of electronic components—protruding upwards from the base. The assembly was mounted in a thermally well insulated, rectangular-sectioned duct, so that air could be sucked solely over the upper *surface of the simulated PCB; the horizontal ribs were arranged to be orthogonal to the horizontal mean air-flow. Steady-state heat-transfer performance data, showing the influence of the geometry of the system, were measured.*

A non-dimensional correlation, which can be used by designers to predict the steady-state rate of heat transfer from such a PCB assembly to the air flow, is

$$\overline{Nu}_C = 1{\cdot}4 \times 10^{-2}\, Re_C^{0{\cdot}88}$$

for $8{\cdot}5 \times 10^2 \leq Re_C \leq 3{\cdot}5 \times 10^4$.

NOTATION

A	Surface area (i.e. top and two sides) of each rib exposed to the air (m^2)
B	Rib protrusion above the base of the simulated PCB (m); see Fig. 1

* To whom all correspondence should be addressed.

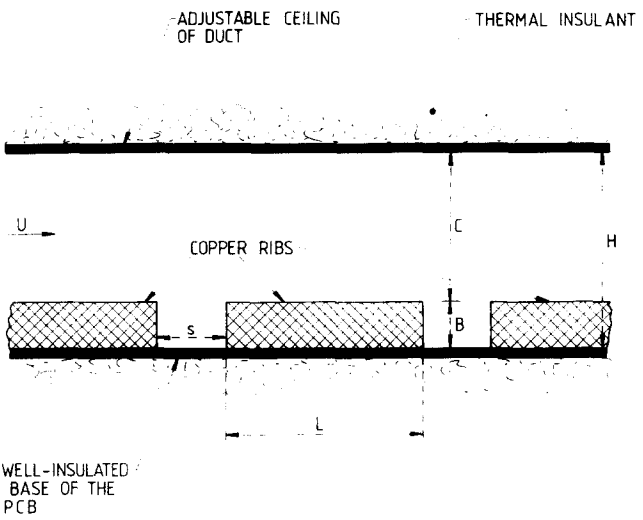

Fig. 1. Vertical axial section showing the geometry and nomenclature of the simulated two-dimensional PCB assembly in the duct: the horizontal ribs (representing the electronic components) stretch almost completely across the duct.

C Clearance between each rib and the ceiling of the duct (m) ($= H - B$); see Fig. 1

c_1, c_2 Constant coefficients in eqns (6) and (7), respectively

E Electric power supplied to each rib (W)

F View factor for thermal radiation from a rib to its surroundings

H Vertical free height within the unencumbered duct (m); see Fig. 1

h Local convective coefficient for heat transfers from a rib to the air-flow ($W m^{-2} K^{-1}$)

$\bar{h}$ Overall mean value of h for all the ribs ($W m^{-2} K^{-1}$)

k Thermal conductivity of the air at temperature T_i ($W m^{-1} K^{-1}$)

L Width of a rib, i.e. dimension in the direction of the mean air-flow (m); see Fig. 1

m, p Power indices; see eqns (6) and (7)

Nu_C Local Nusselt number for heat transfers from the upper surface of the simulated PCB ($= hC/k$)

$\overline{Nu}_C$ Average value of Nu_C over the whole of the upper surface of the simulated PCB

n Number of the (parallel) PCB rib stretching almost the whole width across the duct, except for an air gap of less than 1·0 mm between each vertical end of a rib and the duct wall: $n = 1, 2, 3, \ldots 12$, starting from the leading edge of the PCB

Pr Prandtl number of the air-flow

$\dot{Q}$ Steady-state rate of heat loss from the simulated PCB (W)

Re_C Reynolds number for the air-flow ($= UC/\nu$)

s Uniform spacing between successive ribs (m); see Fig. 1
T_i Mean steady-state temperature of the air at the inlet to the test section (K)
T_s Mean steady-state temperature of the surfaces of the ribs which are exposed to the air (K)
U Mean speed of the air in the duct ($m\,s^{-1}$); see Fig. 1
ε Mean emissivity of surfaces of the ribs with respect to thermal radiation
ν Kinematic viscosity of the air at temperature T_i ($m^2\,s^{-1}$)
σ Stefan–Boltzmann constant ($W\,m^{-2}\,K^{-4}$)

Subscripts

C Based upon the rib-to-duct clearance; see Fig. 1
conv Via forced convection
H Based upon the vertical height of the unencumbered duct; see Fig. 1
i Of the air, at entry to the test section
lenv Via conduction
n For the nth rib
rad Via thermal radiation
s Of the rib's surfaces
w For the walls of the duct

HOW TO ACHIEVE THE REQUIRED COOLING EFFECTIVELY

The miniaturisation of semiconductor components and the increasing use of compact integrated circuit-boards has resulted in local power densities for PCBs rising recently by much as 30% per year. The associated local rates of heat flux, which must be dissipated to the ambient environment, have increased dramatically in order to avoid the overheating of the electronic components, so ensuring better reliability. The prime aim is to keep the temperatures of the electronic components well below the maximum service-temperature (i.e. normally $<65°C$) because their mean times-to-failure are usually halved, at least, by each 10°C rise thereafter.

For many applications, sufficient cooling of electronic systems can be achieved primarily by natural convection, which is usually silent in operation and cheap. Nevertheless, the design should be optimised, thereby ensuring that maximum cooling will occur for a chosen financial investment. However, natural convention is usually the weakest mechanism for expelling rapidly the heat generated within electronic components[1–4] (see Fig. 2). Where this approach is deemed to be inadequate, more vigorous cooling

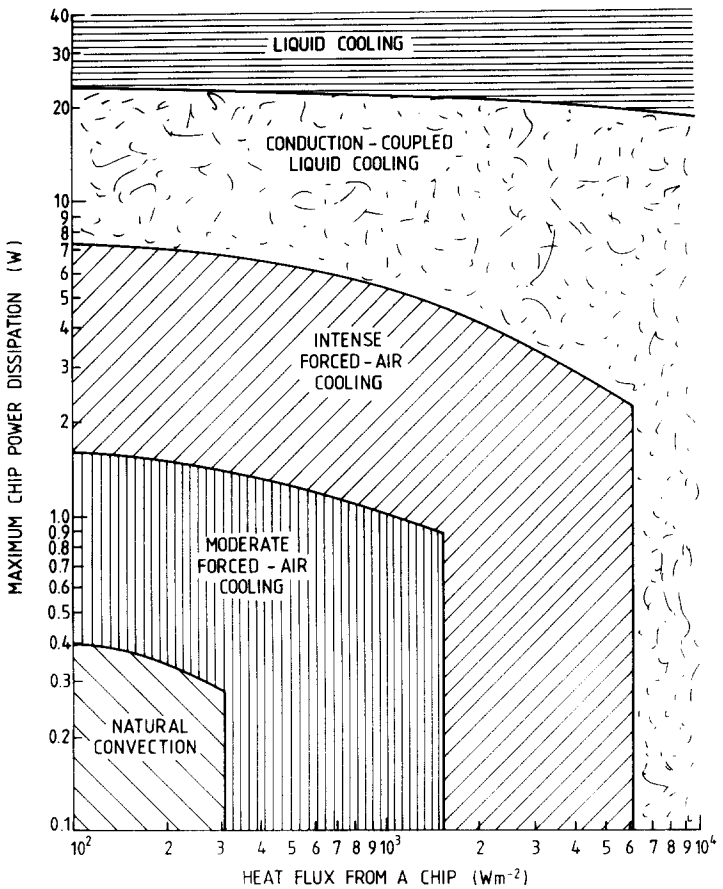

Fig. 2. Approximate classification of the zones of appropriate applicability for commonly employed cooling techniques.[4]

mechanisms, such as forced convection, are employed. However, wherever feasible, direct air-cooling is preferable (to liquid cooling, for example) because of the ready availability of air and the simplicity of the system that is then required. Direct air-cooling is therefore frequently used in conjunction with electronic devices, such as personal computers, in order to achieve acceptable performances.

Figure 3 shows an example of a commonly used arrangement for a small electronic cabinet containing several PCBs. Each board has its electronic components mounted in aligned arrays, and several such boards are usually stacked. Each parallel channel between neighbouring PCBs has a relatively rough lower surface (i.e. the electronic-component side), above which is a relatively smooth surface (i.e. the lower surface of the superimposed neighbouring board). The heat transfers which occur include conduction

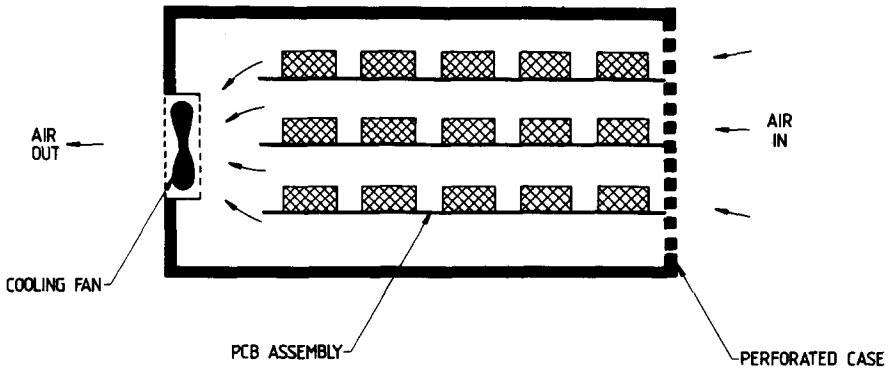

Fig. 3. Typical forced air-cooling system for an electronic cabinet.

from the heat-dissipating electronic components to the boards, as well as conduction, convection and radiation from the PCB assembly to the surroundings. For the assembly under investigation, most (>95%) of the thermal energy dissipated in the simulated electronic components is removed by the cool air being sucked over them.

RELATED LITERATURE

Scott's succinct guide[1] introduced a simple analytical method for predicting the behaviour of cooling systems for electronic devices. More recently, Incropera[2] and Peterson & Ortega[3] presented comprehensive reviews of the same subject. Incropera recommended, in particular, that further studies should be undertaken to determine the effects of the geometries of such electronic devices on the rates of forced convective heat transfers that occur from them (hence the present investigation was undertaken). For the same purpose, Peterson & Ortega discussed analytical, numerical and experimental studies concerning natural and forced convection; boiling and immersion cooling; thermal contact-resistance; and the use of heat pipes.

Oktay *et al.*[4] considered the thermal management of electronic packages, and hence the cost-effective use of forced convective air-cooling. Arvizu & Moffat[5] determined for the steady-state heat losses from a regular array of duralumin cubes subjected to convecting air (see Fig. 4): the heat-transfer coefficient rose as a result of decreasing the channel width for a fixed cube-size and inlet-air speed. A superposition approach, for calculating the temperature distribution in the array, was also developed. However, the side dimension of the duralumin cubes was 13 mm: this well exceeds the usual protuberance of chips in practice.

Lehmann & Wirtz[6,7] undertook flow visualizations, using smoke, in a

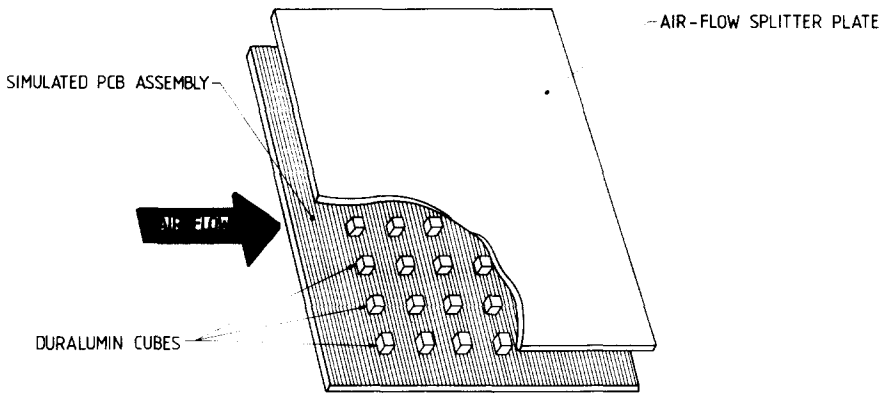

Fig. 4. The experimental rig of Arvizu & Moffat;[5] a simulated PCB assembly, with a uniformly spaced array of duralumin cubes mounted on an insulating board.

channel containing uniformly spaced rectangular ribs. It was concluded that the steady-state rate of convective heat-transfer was insensitive to changes the value of H (see Fig. 1). For small spacings of the ribs, i.e. $s/L = 0{\cdot}25$, the air currents between adjacent ribs and the base did not noticeably influence the rate of heat transfer from the top surface of the downstream rib. However, significant effects occurred when $s/L \geq 1{\cdot}0$. It was also suggested that only laminar flow occurred when the Reynolds number, Re_H, for the flow, based on the vertical height of the unencumbered duct, was less than 1000, and that transitional flow persisted for values of Re_H up to 2000. All the results were obtained with a single rib size, i.e. $L = 500$ mm and $B = 12{\cdot}5$ mm, so the effect of a variation in the ribs' dimensions on the convection was not ascertained. Tewari & Jaluria[8] investigated the mixed free-and-forced convective heat transfers from thermal-energy sources mounted on horizontal or vertical surfaces.

Bayazitoglu & Davalath[9] simulated numerically the convective heat transfers from three heated rectangular blocks. The incompressible flow was modelled using the fully elliptic forms of the Navier–Stokes equations. A control-volume-based finite-difference procedure was implemented. Predictions were made of the optimal value of the spacing, between successive ribs, which resulted in the maximum rate of heat dissipation from the system being achieved.

Anderson & Moffat[10] assessed critically the options available for defining the local heat-transfer coefficient with respect to various reference temperatures, namely, (1) the *free-stream* temperature (i.e. that remote from the heated surface); (2) the *mixed-mean* temperature (obtained from the energy-balance equation); (3) the *channel-inlet* temperature (i.e. that of air at the inlet to the test section); and (4) the *adiabatic* temperature (i.e. the

temperature of the non-directly-heated component, when the other components are being energised). The superposition method was applied to analyse the thermal performance of the PCB assembly: the method could account for the effect of varying the heat flux from component to component.

Patankar & Schmidt[11] performed extensive numerical analyses of the heat transfers which occur in the fully developed region of a duct containing heated, unformly spaced blocks under laminar-flow conditions. Three systems were investigated: the blocks were located either on one side or on both sides, in either symmetric or staggered arrangements. Computations were undertaken for

$$\frac{s+L}{H} = 1{\cdot}0,\ 1{\cdot}25,\ 1{\cdot}50 \text{ or } 2{\cdot}0$$

$$\frac{L}{H} = 0{\cdot}5,\ 0{\cdot}667 \text{ or } 1{\cdot}0$$

and

$$\frac{B}{H} = 0\text{–}0{\cdot}667$$

Abbound *et al.*[12] performed experimental studies and numerical analyses concerning the forced convective cooling of dual-in-line packages mounted on boards to form a multichannel flow, i.e. with several boards stacked in parallel. Unfortunately, the interesting data were limited to those for a single board size and orientation.

EXPERIMENTAL

The experimental system (Fig. 5)

The system for thermally simulating the behaviour of a PCB for this investigation consisted of 12 upward-facing, highly polished, rectangular ribs, made from uniformly sized, reactangular copper bars, mounted with uniform spacings on a horizontally orientated smooth board. The heated ribs, which were intended to simulate the thermal behaviour of the electronic components at slightly above ambient temperatures, were highly polished in order to achieve a surface emissivity of less than 0·3 (as indicated by a Minolta 505 infrared spot thermometer). Thus the thermal-radiation contributions to the rates of heat loss from the simulated PCB were relatively small ($<5\%$), so it could be assumed that the heat generated within the ribs was deliberately lost primarily by the forced convective air-

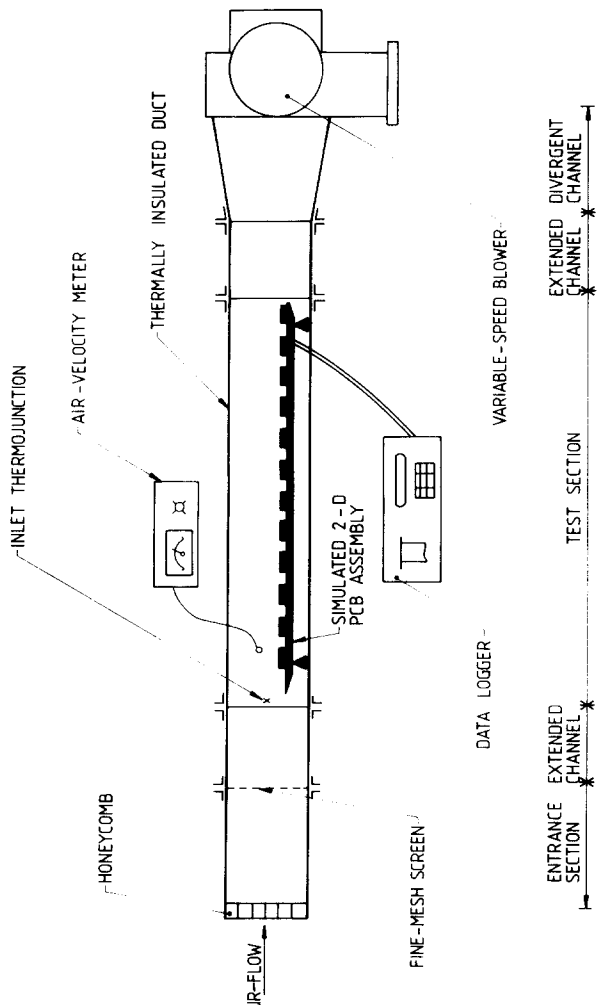

Fig. 5. Schematic diagram of the experimental set-up: using the notation introduced in Fig. 1, $B = 6{\cdot}35$ mm; $s = 6{\cdot}35$ mm; $L = 19{\cdot}05$ mm or 25·4 mm; $H = 12{\cdot}7$ mm, 25·4 mm, 50·8 mm or 6·5 mm.

flow. The simulated board was a mica sheet 200 mm wide and 2 mm thick, fixed to a bakelite substrate 6·35 mm thick, the undersurface of which was covered with a layer of fibreglass. The board was machined to have sharp leading and trailing edges in order to try to reduce the production of local turbulence in the air-flow.

Two very thin heater strips, each of 200 mm length and 0·8 Ω resistance, were embedded in the base of each copper rib, so that the base of the rib could be heated reasonably uniformly. A thermojunction and associated leads were embedded in a narrow central slot (orthogonal to the mean air flow) in the upper surface of each rib; the residual cavity was filled with cold-setting Araldite, so that the resulting surface was flat, smooth and flush with the upper surface of the rib. The leads were fed out through the vertical wall (exactly adjacent to the rib) of the wind tunnel. The thermocouple signals were converted to temperature readings via a Fluke 2190A digital voltmeter.

The simulated PCB was placed symmetrically in the wind tunnel's rectangular test section (length 600 mm, width 202 mm and maximum height 120 mm) made of Bakelite sheet 6·35 mm thick. The whole test section was thermally insulated externally by glass-fibre 50 mm thick. The internal height, H, of the wind tunnel (see Fig. 1) was varied, so that $H/B = 2, 4, 6, 8$ or 10.

The air was sucked through the wind tunnel by a National Mini-Sirocco™ blower whose power could be altered via a variable-voltage transformer, so that $2\,\mathrm{m\,s^{-1}} < U < 10\,\mathrm{m\,s^{-1}}$. The mean air-flow speed, U, was measured with a Kurtz 441 M meter. Uniformity of the air-flow was achieved by passing it through a honeycomb (constricted of 12·7 mm × 12·7 mm × 76·2 mm duralumin tubes) and then through a fine bronze-wire mesh screen having 100 holes $\mathrm{cm^{-2}}$.

Data handling and interpretation

The rate of heat loss, by forced convection from each rib, is

$$\dot{Q}_{\mathrm{conv}} = \dot{E} - \dot{Q}_{\mathrm{rad}} - \dot{Q}_{\mathrm{lenv}} \tag{1}$$

where the rate of radiation loss, $\dot{Q}_{\mathrm{rad}}$, from each rib was only a small fraction (< 5%) of the electric power, $\dot{E}$, consumed in that rib. The value of the conductive loss, $\dot{Q}_{\mathrm{lenv}}$, from the rib to the simulated substrate was assessed from a knowledge of the thermal conductivities of the materials and the measured associated temperature-distribution. The values were such that $\dot{Q}_{\mathrm{lenv}}$ was always small (i.e. almost negligible) for this series of experiments. The rate of thermal radiation loss, $\dot{Q}_{\mathrm{rad}}$, from a rib to its environment was estimated using the Stefan–Boltzmann equation:

$$\dot{Q}_{\mathrm{rad}} = \sigma A F \varepsilon (T_{\mathrm{s}}^4 - T_{\mathrm{i}}^4) \tag{2}$$

where the view factor, F, for the rib in its surroundings, was taken to be unity and the surface emissivity $\varepsilon \approx 0{\cdot}3$.

For each steady-state set of experimental observations, the value of $\dot{E}$ was measured, together with the appropriate temperatures, and the corresponding values of $\dot{Q}_{\text{rad}}$ and $\dot{Q}_{\text{lenv}}$ deduced. Hence the value of $\dot{Q}_{\text{conv}}$ was determined. Then the convective coefficient for heat transfers from rib n to the air-flow was obtained from the definition

$$h_n = \frac{\dot{Q}_{\text{conv}}}{A(T_s - T_i)} \tag{3}$$

where the steady-state temperature, T_i, of the air at the inlet of the test section (see Fig. 5) was used as the reference temperature. The overall heat-transfer coefficient $\bar{h}$ of the simulated PCB assembly was deduced from

$$\bar{h} = \frac{1}{12}\sum_{1}^{12} h_n \tag{4}$$

where n is the row numer of the considered rib ($n = 1, 2, 3, \ldots, 12$).

In defining the Reynolds and Nusselt numbers for the air-flow, the vertical clearance $C\,(= H - B)$ (see Fig. 1) was chosen as the characteristic dimension. Also, for this purpose, the thermal properties of air were evaluated at the temperature, T_i, of the inlet air; the speed, U, of the air was taken as the r.m.s. average value at the central location for the inlet to the test section. For the simulated PCB, the overall Nusselt number

$$\overline{Nu}_C = \frac{1}{12}\sum_{1}^{12} Nu_C = \frac{\bar{h}C}{k} \tag{5}$$

The dimensionless parameters used to describe the heat transfer between the simulated PCB and the air-flow were related in the traditional way, viz.

$$\overline{Nu}_C = c_1 \mathrm{Re}_C^m Pr^p \tag{6}$$

Because the Prandtl number for air in the considered temperature range remained almost constant (i.e. $\sim 0{\cdot}707$), eqn (6) could be simplified to become

$$\overline{Nu}_C = c_2 Re_C^m \tag{7}$$

Observations and measurements

The presence of the first five ribs (across the air-stream) was sufficient to ensure that thereafter, further downstream, the hydrodynamic boundary-layer was fully developed.

Steady-state rates of forced convective heat transfer from the heated

simulated PCB to the relatively cold air-stream being sucked over its upper surface, and the associated temperature distributions, were measured. Representative data, deduced from a vast number of experimental observations, are plotted in Figs 6–10.

Deductions

The ability of a particular rib, or the whole simulated PCB, to dump heat rapidly is dependent upon the following parameters.

1 Which rib row is considered

The local steady-state rate of heat transfer was greatest for the first rib, and thereafter decreased for each subsequent rib row until it became almost row-independent (i.e. as for row 10). The thermal boundary layer became progressively thicker (i.e. the local heat-transfer coefficient was reduced), the further it was from the leading edge, until fully developed flow was achieved. However, an increase in the local heat-transfer coefficient occurred for the last rib (i.e. row 12): this is due to the 'exit' effect, i.e. the sudden enlargement of the flow aperture soon after row 12, resulting in rises in the local air speeds around rib 12.

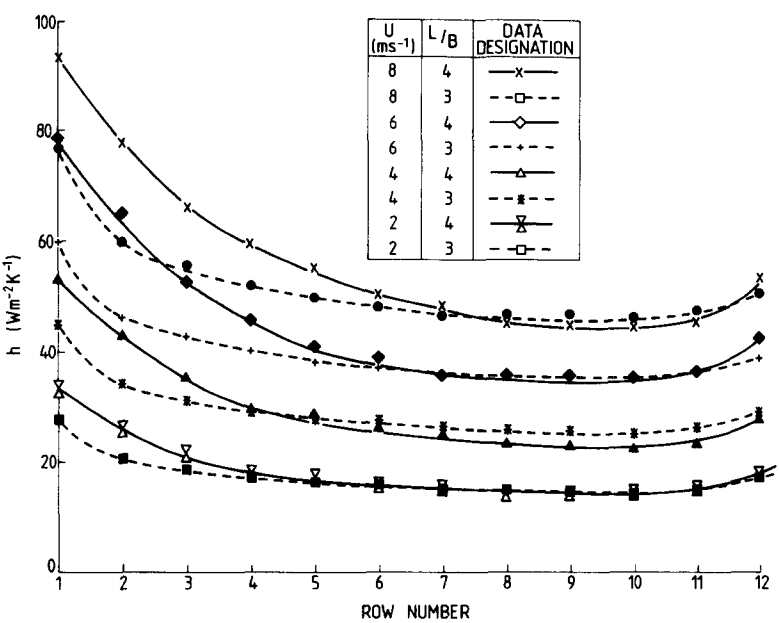

Fig. 6. The variation of the *local* heat-transfer coefficient for the uniformly spaced copper ribs stretching almost completely across the air-stream: $H/B = 10$. Row 1 is near the leading edge of the board, and the ribs are numbered successively towards the trailing edge.

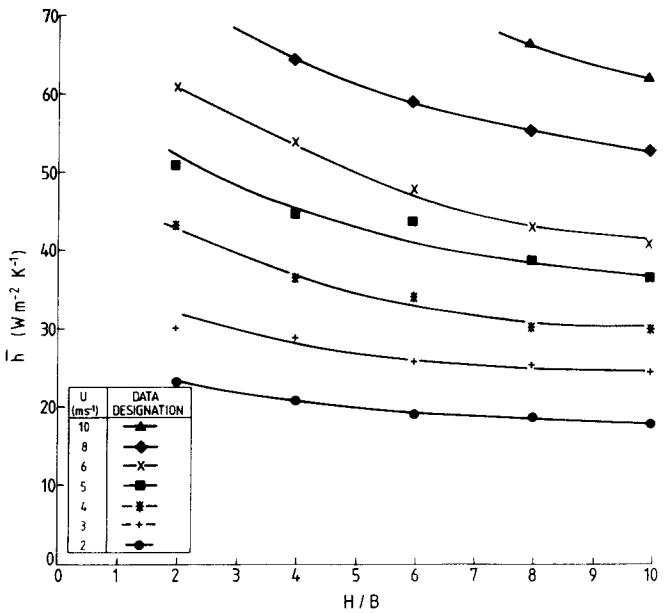

Fig. 7. Effect upon the overall heat-transfer coefficient of varying the H/B ratio; $L/B = 3$.

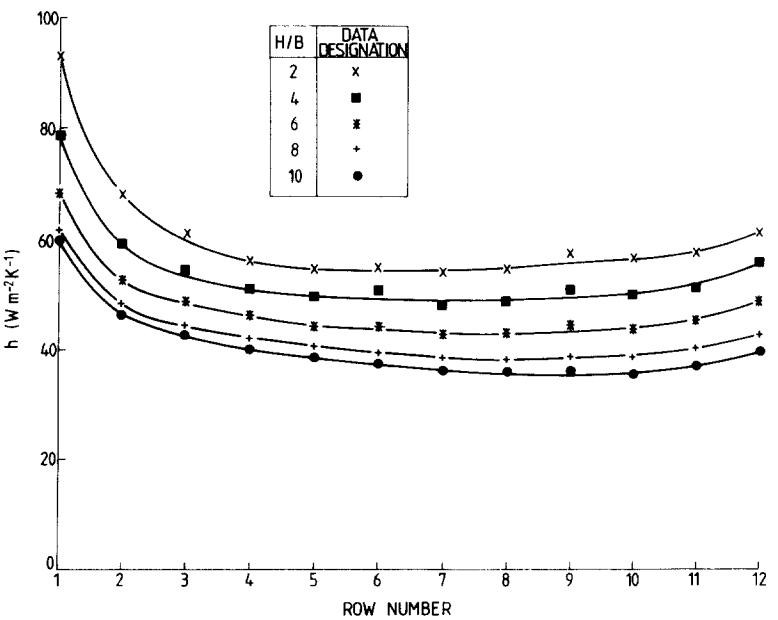

Fig. 8. Variation of the local heat-transfer coefficient with the row number (of the ribs) along the board; $L/B = 3$ and $U = 6\,\mathrm{m\,s^{-1}}$. By row 10 h is almost independent of the row number.

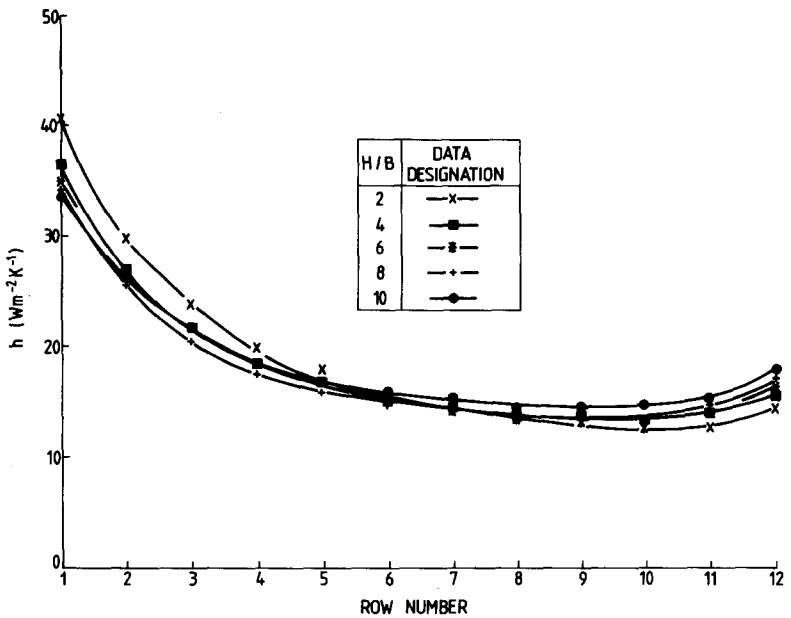

Fig. 9. Variation of the local heat-transfer coefficient with the row number (of the ribs) along the board; $L/B = 4$ and $U = 2\,\mathrm{m\,s^{-1}}$.

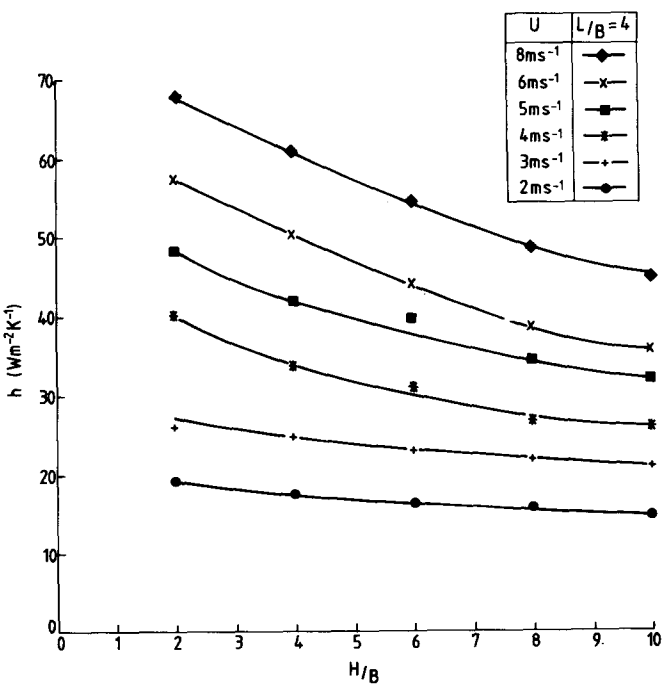

Fig. 10. Variation of the local heat-transfer coefficient with the H/B ratio. $L/B = 4$.

2 Mean air speed

The heat-transfer rate from the simulated PCB could be enhanced by increasing the value of U but, in practice, there will be limits (e.g. because of cost) to the size and power of the blower (or fan) which will be adopted.

3 Channel height, H

When the mean air-speed, U, and rib dimensions remained invariant, the value of $\bar{h}$ decreased as H was increased. However, if the value of H was relatively large, the local heat-transfer coefficient, h, tended to be invariant, irrespective of the value of H. When $H/B \geq 8$, the rate of heat transfer from the upper (i.e. horizontal) surface of each rib exceeded that from the rib's (vertical) sides.

As the value of H was decreased, the relative effective roughness of the channel rose, so that the resulting enhanced turbulence led to a higher rate of forced convective heat transfer. The strength of the air recirculation within each slot, between adjacent ribs and the board, also increased and so enhanced rates of heat transfer from the exposed sides of each rib ensued. In addition, narrowing the duct increased the air-flow speed across the top of each rib. The combination of these effects produced an increased rate of heat transfer from the simulated PCB as the value of the ratio H/B was reduced. As the channel then became more constricted, the blower (or fan) power expended for maintaining the same value of U had to be changed approximately. The increase in the heat-transfer rate obtained by reducing the channel height became less significant for large values of L and low values of U.

The present conclusions concerning the influence of the value of H on the values of h and $\bar{h}$, which have been obtained solely with L equal to 19·05 mm, agree well with those of Arvizu & Moffat.[5] Lehmann & Wirtz[6] observed that the variation in the value of H would produce less effect on the convection, the greater the value of L: this was corroborated by the present investigation when $L = 25{\cdot}4$ mm. As a result of increasing the value of H, the values of all the other parameters remaining invariant, (a) the number of rows of ribs from the leading edge of the simulated PCB required for a fully developed thermal boundary layer to be established was increased, and (b) the value of the 'row-independent' local heat-transfer coefficient decreased.

4 Width, L, of each rib

As L increased, the values of all the other variables remaining invariant the following changes occurred: (a) the number of rows from the leading edge required for the air-flow to achieve its fully developed behaviour also increased; and (b) the magnitude of the row-independent heat-transfer coefficient decreased, because the thermal boundary layer over the top of

each rib grew. The latter corroborates the conclusion of Patankar & Schmidt.[11] The benefit of using a lower value of L diminished as H increased.

5 Extents of the developing and fully developed boundary layers

The overall heat-transfer coefficient for the simulated PCB is an average of the local heat-transfer coefficients for the ribs; some experience the developing and others the fully developed boundary layer.

The values of the overall heat-transfer coefficient, $\bar{h}$, for the simulated PCB for various values of H and for two values of rib width L employed, i.e. 19·05 and 25·4 mm show that a change of preference (i.e. in order to obtain a higher value of $\bar{h}$) occurs when selecting the width, L, of the rib for the vaious values of H and U (see Fig. 11).

For small values of H, more of the simulated PCB will experience a fully developed boundary layer: then the row-independent local heat-transfer coefficient is close in magnitude to the overall heat-transfer coefficient. For channels with high values of H, the air-flow travels a longer distance from the leading edge before a fully developed boundary layer occurs over the PCB: then the value of $\bar{h}$ is greater.

The relative extents of the developing and fully developed boundary layer regions above the PCB are also influenced by the number, n, of the rows of

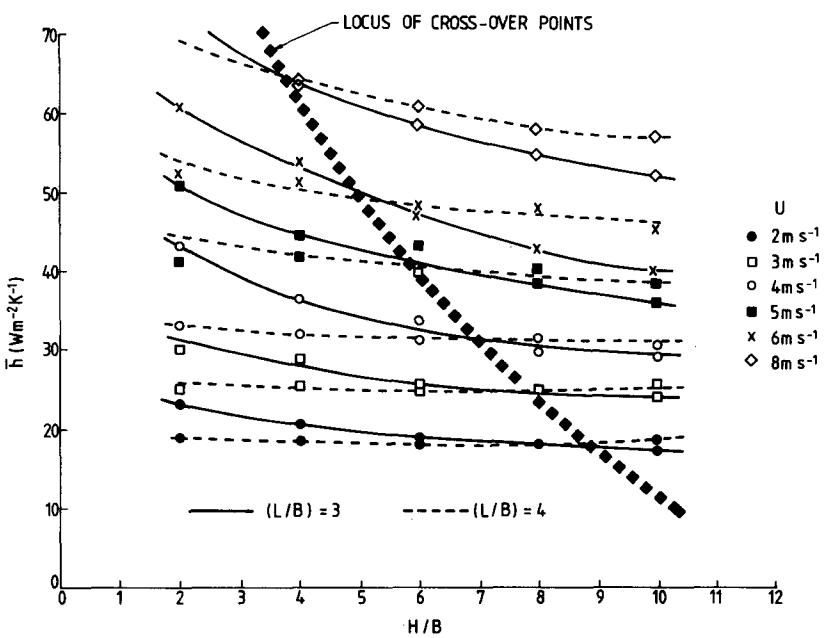

Fig. 11. Variation of the overall heat-transfer coefficient for the simulated PCB for $L/B = 3$ or 4 and various H/B ratios.

ribs on the board. The locus of the cross-over points on Fig. 11 will be shifted to smaller H/B ratios as n rises. For a long board (i.e. large in the direction of the mean air-flow) with a large number, n, of ribs, each of relatively narrow width (i.e. a small value of L), the magnitude of the overall heat-transfer coefficient, $\bar{h}$, will become closer to the row-independent value.

Correlation of the experimental data

The experimental data were rearranged to form dimensionless groups and are plotted in Fig. 12, although not all the data are shown. The resulting best-fit straight line (for all the data) in the form of eqn (7) was, for $8{\cdot}5 \times 10^2 \leq Re_C \leq 3{\cdot}5 \times 10^4$,

$$\overline{Nu}_C = 1{\cdot}4 \times 10^{-2}\, Re_C^{0{\cdot}88} \tag{8}$$

where the coefficient and the power index have been determined using a

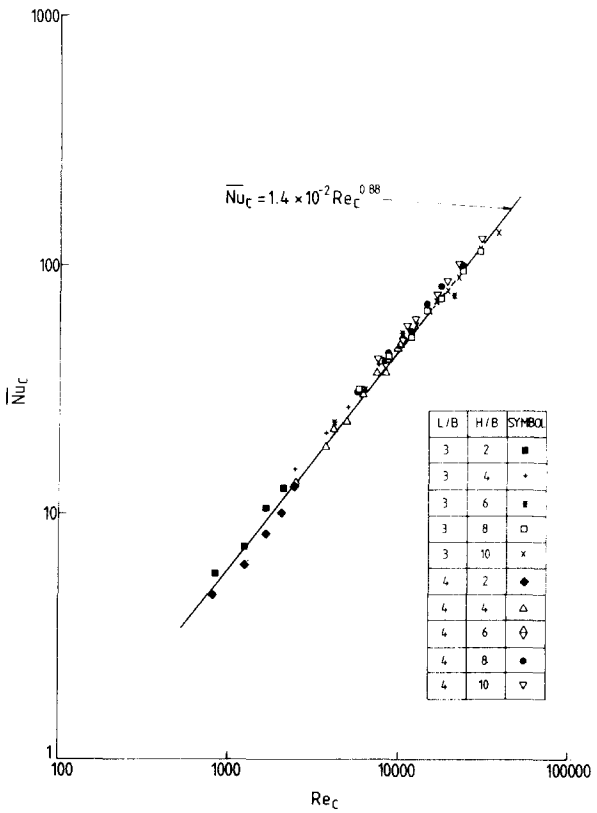

Fig. 12. Overall Nusselt number for the simulated PCB versus the Reynolds number for the air-flow.

least-squares method: the standard deviation from this best fit is $\pm 1{\cdot}17 \times 10^{-2}$.

The boundary layers along the vertical walls of the duct inhibit the flow, and so the rates of heat transfer as indicated by the present correlation would give slightly lower values of $\overline{Nu}_C$ than if two-dimensional flow had occurred over all parts of the ribs. Nevertheless, such boundary-layer inhibitions would occur in PCB assemblies in practice, so the performance indicated by eqn (8) represents a reasonable design guide.

COMMENT

The orientation of the rectangular electronic chips on the PCB relative to the mean forced convective air-flow direction will influence significantly the overall heat-transfer coefficient, $\bar{h}$. For a short PCB, it is preferable for the chips to be aligned *in the direction of* the undisturbed air-flow, because the overall convective heat transfer will be increased by the longer boundary-layer development region which then ensues. However, for a relatively long PCB, as in the present investigation, the rows of chips should be located *transversely* to the air-flow, thereby shortening the development region and leading to a larger row-independent heat-transfer coefficient than for the same location on the board, but with the mean air flow aligned with the channels between the ribs. In general the gaps between the boards should be kept small, but the exact choice will be influenced by the available fan power.

REFERENCES

1. Scott, A. W., *Cooling of Electronic Equipment*. J. Wiley & Sons, New York, 1974.
2. Incropera, F. P., Convection heat transfer in electronic equipment. *J. Heat Transfer*, **113** (1988) 1097–111.
3. Peterson, G. P. & Ortega, A., Thermal control of electronic equipment and devices. *Advances in Heat Transfer*, **20** (1990) 181–314.
4. Oktay, S., Hanneman, R. & Bar-Cohen, A., High heat from a small package. *Mechanical Engineering*, **108** (1986) 36–42.
5. Arvizu, D. E. & Moffat, R. J., The use of superposition in calculating cooling requirements for circuit-board mounted electronic components. *Proc. 32nd Electronic-Components Conf.*, 1982, pp. 133–44.
6. Lehmann, G. L. & Wirtz, R. A., Convection from surface-mounted repeated ribs in a channel flow. ASME Paper, No. 84-WA/HT-88, 1984.
7. Lehmann, G. L. & Wirtz, R. A., The effect of variations in stream-wise spacing and length on convection from surface-mounted rectangular components. HTD-48 ASME, New York, 1985, pp. 39–47.
8. Tewari, S. S. & Jaluria, A., Mixed-convective heat transfers from thermal

sources mounted on horizontal and vertical surfaces. *J. Heat Transfer*, **112** (1990) 975–87.
9. Bayazitoglu, Y. & Davalath, J., Forced-convection cooling across rectangular blocks. *J. Heat Transfer*, **109** (1987) 321–8.
10. Anderson, A. M. & Moffat, R. J., Applying heat-transfer coefficient data to electronic cooling. *J. Heat Transfer*, **112** (1990) 882–90.
11. Patankar, S. V. & Schmidt, R. C., A numerical study of laminar forced-convection across heated blocks in two-dimensional ducts. ASME Paper No. 86-WA/HT-88, 1986.
12. Abbound, H., Hardisty, H. & Vertman, S., Forced-convection air cooling of an array of electronic modules using the finite-element method to analyze module heat-transfer. *Proc. Inst. Mech. Engrs*, **202** (1988) 321–32.